PHOTONIC ANALOGUE-TO-DIGITAL CONVERTER BASED ON WAVELENGTH DIVISION MULTIPLEXING TECHNIQUE

Tiago Alves and Adolfo Cartaxo

Group of Research on Optical Fibre Telecommunication Systems, Instituto de Telecomunicações, DEEC
Instituto Superior Técnico, Av. Rovisco Pais 1, 1049-001, Lisboa, Portugal

Keywords: Photonic analogue-to-digital converter, Time stretching, Ultra wideband, Wavelength division multiplexing.

Abstract: A photonic (Ph) analogue-to-digital (ADC) converter architecture based on the wavelength division multiplexing (WDM) technique used to provide compressed spectrum of the ultra wideband radio signals that are being used in a given pico-cell area for monitoring purposes is presented. The signal at the different points of the WDM Ph-ADC architecture is analyzed and discussed in detail. The advantages/disadvantages of the WDM architecture are identified and compared with its time division multiplexing (TDM) counterpart.

It is shown that the WDM Ph-ADC architecture provides adequate time stretching of the wireless signals captured in a given pico-cell. This system enables relaxing the bandwidth requirements of the electrical ADCs used to digitize the wireless signals prior digital signal processing is applied for spectrum and transceivers localization monitoring. In addition, it is concluded that the WDM Ph-ADC architecture supports higher pulse repetition rates than the TDM Ph-ADC architecture being of special interest when a fast up-date of the radio channel monitoring is required.

1 INTRODUCTION

The photonic (Ph) analogue-to-digital converter (ADC) system was initially proposed as a powerful solution to provide time-stretching/frequency-compression of high frequency signals in order to relax the electrical receivers bandwidth (Han and Jalali, 2003).

Recently, a multi-channel Ph-ADC system based on time division multiplexing (TDM) technique has been proposed (Llorente et al., 2008; Llorente et al., 2009; Alves and Cartaxo, 2011). This Ph-ADC system is used to compress the spectrum of ultra-wideband (UWB) radio signals captured from sensor antennas that are strategically located inside home premises. From this compression, spectrum monitoring, fingerprinting and localization of the different UWB transceivers that are being used in a given pico-cell can be performed by digital signal processing (DSP) techniques. The main advantage of such Ph-ADC system is the relaxed requirements of the electronic ADCs (E-ADC) used to monitoring the whole UWB band (from 3.1 until 10.6 GHz). In this paper, a Ph-ADC based on the wavelength division multiplexing (WDM) technique is proposed for the first time

(to the best of our knowledge). The operational limits of the WDM Ph-ADC architecture are analyzed through numerical simulation and discussed in detail. The main advantages/disadvantages of this architecture when compared with the TDM-based architecture are also identified.

2 WDM PH-ADC ARCHITECTURE

2.1 System Description

Fig. 1 depicts the setup diagram of the WDM Ph-ADC architecture. The optical source may be implemented using a super continuum (SC) source generating an optical pulsed signal with a flat wideband spectrum. This spectrum is then filtered (for instance, using an arrayed waveguide grating (AWG)) in several slices (as much as the number of sensors used to acquire the electrical signals from the radio interface in a given room scenario), multiplexed and launched into a dispersive spool of fibre in order to stretch the time signal waveforms. After the fibre,
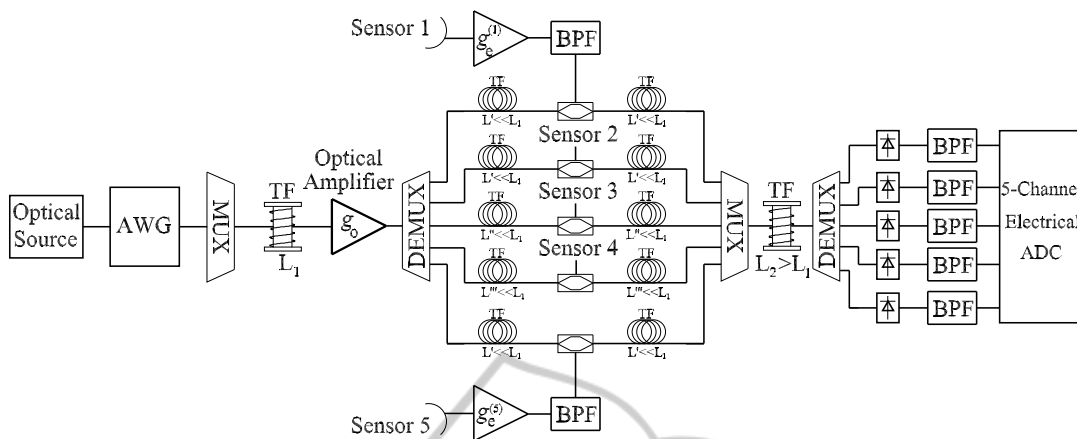
Figure 1: Schematic diagram of the photonic part of the WDM Ph-ADC architecture.

the different optical pulsed signals (each one centred at a different optical wavelength) are demultiplexed and used to feed each electro-optic modulator (EOM) that is located in each sensor antenna. The wireless signals acquired in each sensor antenna are then used to modulate the respective optical pulsed signal. It should be highlighted that, with this architecture, the electrical signal snapshots acquired by the different sensors antennas in a given time instant are converted to the optical domain at the same time instant (apart the walk-off between the different wavelengths resulting from the propagation along the first spool of fibre) using optical pulsed signals transmitted at different wavelengths. Instead, in the TDM architecture, only one wavelength is used and the snapshots of the different sensors are transmitted separately in time. The optical pulsed signals are then multiplexed and launched into the second spool of fibre. After achieving the proper time stretching (TS) by adequate adjustment of the dispersion of the first and second spool of fibres, the optical signals carried in the different wavelengths are demultiplexed and the electrical signals snapshots are obtained using positive-intrinsic-negative (PIN) photo-detectors. The detected electrical signals are band-pass filtered (to reduce the low frequency/high power spectrum due to the optical pulsed signal) and applied to the E-ADC card where DSP is accomplished. From the comparison of the WDM with the TDM Ph-ADC architecture presented in (Alves and Cartaxo, 2011), the following outcomes are drawn: a wider band optical source is required in the WDM than in the TDM architecture; ii) the WDM architecture may be more expensive than the TDM as it requires additional optical devices as multiplexers (MUXs), demultiplexers (DEMUXs) and PIN photo-detectors, and electrical devices as band-pass filters (BPFs) and electrical amplifiers and iii) the WDM architecture requires a

multi-channel E-ADC card as the signals may arrive to the card simultaneously. The main advantage of the WDM architecture over the TDM one is related to the possibility of having a higher pulse frequency rate that enables faster up-dating on the fingerprinting, localization and power levels control of the UWB transceivers used in a given pico-cell.

2.2 Description of the WDM Ph-ADC System Parameters

The analysis of the WDM Ph-ADC architecture is accomplished considering similar parameters to the ones used in (Alves and Cartaxo, 2011) for the TDM Ph-ADC architecture. Particularly, it is considered that:

- The arrayed waveguide grating is characterized by a Gaussian transfer function (in order to have optical time pulsed signals with a Gaussian shape) with a -3 dB bandwidth of 1.7 nm.

- The time stretching factor is 3.4 (and consequently the fibre spools lengths are the same as for the TDM solution) in order to meet the time aperture specifications mentioned in (Alves and Cartaxo, 2011).

- The electro-optic conversion is performed by conventional Mach-Zehnder modulator biased at the quadrature point.

- The electrical and optical amplifiers present the same noise characteristics to the ones considered in (Alves and Cartaxo, 2011).

- A 6-*th* order band-pass Bessel filter with a -3 dB bandwidth of 13 GHz and with maximum amplitude response at 5.48 GHz is used in each sensor to model the limited bandwidth of the electrical noise and a 6-*th* order band-pass Bessel filter with
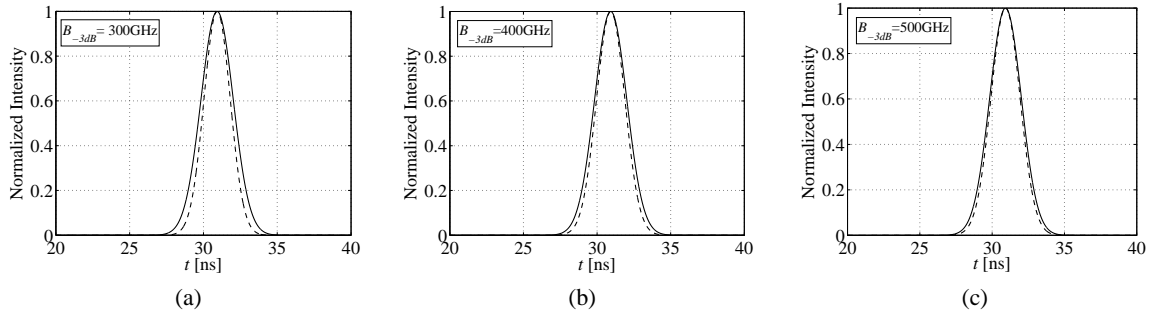
Figure 2: Normalized intensity of the optical pulses at the DEMUX input (continuous line) and the DEMUX output (dashed line).

a -3 dB bandwidth of 1.4 GHz and with maximum amplitude response at 1.1 GHz is used at the PIN output.

- The transmission over the first and second spools of fibre is linear.

However, the pulse repetition rate used in the WDM architecture is five times higher than the one used in the TDM architecture presented in (Alves and Cartaxo, 2011) - 3.23 MHz - as the optical pulses are not multiplexed in time.

3 WDM PH-ADC ARCHITECTURE OPERATION IN THE ABSENCE OF ELECTRICAL SIGNALS

The appropriate operation of the WDM Ph-ADC architecture is limited mainly by two parameters: the optical channel spacing used between the different optical transmitted channels and the bandwidth of the MUXs/DEMUXs used to combine/separate those optical channels. In this section, a brief study on the impact of these parameters on the WDM Ph-ADC architecture is accomplished. To simplify the analysis, no electrical signals applied to the EOM are considered.

3.1 Bandwidth of MUXs/DEMUXs

In this work, the absence of (or negligible) time waveform differences between the signals before and after the MUXs/DEMUXs operation is considered as a criterion to identify the most adequate bandwidth for these devices. This criterion is used in order to obtain low distortion induced by the 2 MUXs and 2 DEMUXs chain of the WDM Ph-ADC system on the time waveform. The study is accomplished by taking

into account the WDM Ph-ADC system described in section 2 and considering the transmission of only one optical pulsed signal (obtained by proper filtering of the flat spectrum generated by the SC source) in order to avoid inter-channel crosstalk.

Fig. 2 shows the normalized intensity of one optical pulse at the DEMUX (located after the first spool of fibre) input and output for different -3 dB bandwidth values of the DEMUX Gaussian shape. Fig. 2 shows that tight bandwidths decrease the time aperture of the optical pulse. It is also shown that although the optical pulse remains almost unchanged for a bandwidth of 500 GHz, the reduction of the pulse time aperture cannot be neglected anymore for a bandwidth of 300 GHz. For the 400 GHz bandwidth case, a slight reduction of the time aperture is also observed. Nevertheless, this reduction is not much significant and the 400 GHz bandwidth case is preferable (when compared with 500 GHz) as it allows for lower optical channel spacing in the WDM architecture and, consequently, for lower optical bandwidth requirements in the WDM Ph-ADC system. Hence, in this work, the -3 dB bandwidth of the MUXs/DEMUXs used along the optical path is set to 400 GHz.
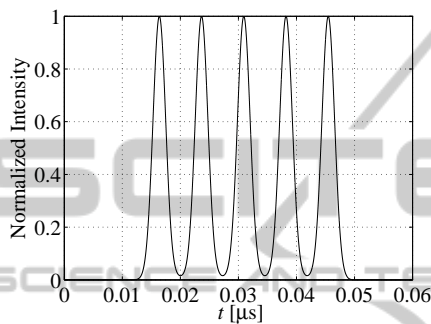
3.2 Optical Channel Spacing

Due to the very large bandwidth of each optical signal used to "sample" the radio signals captured by the sensors antennas, the walk-off induced by the fibre on each WDM channel may be of special relevance and its impact on the system operation should be carefully analyzed. The study of the influence of the optical channel spacing on the WDM operation is accomplished by considering the Ph-ADC architecture comprising five sensors as depicted in Fig. 1.
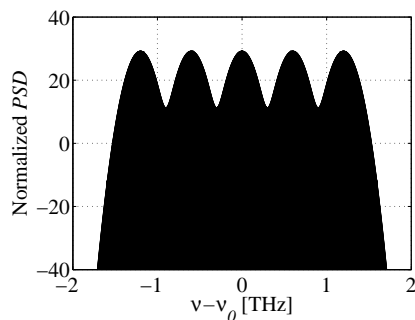
Fig. 3 depicts the time waveform and the power spectral density (PSD) of the multiplexed signal at the output of the first spool of fibre considering an optical channel spacing of 600 GHz. Fig. 3(b) shows a
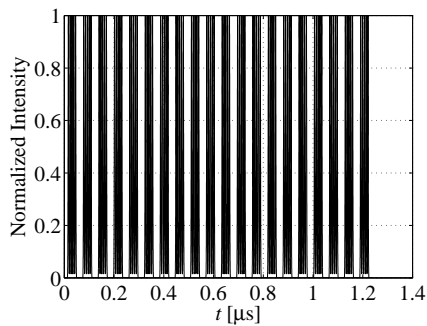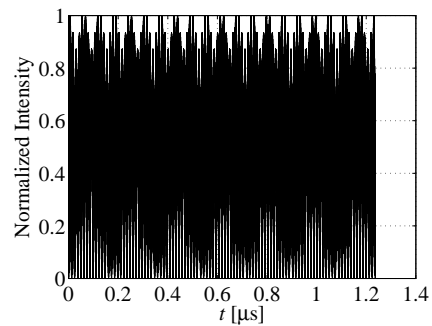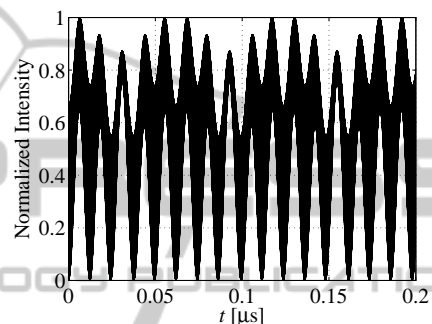
(a)

(b)

(c)

Figure 3: a) Multiplexed optical pulses at the output of the first spool of fibre. b) Zoom of a). c) PSD of the multiplexed signal represented in a). Results obtained for an optical channel spacing of 600 GHz.

(a)

(b)

Figure 4: a) Multiplexed optical pulses at the output of the second spool of fibre. b) Zoom of a). Results obtained for an optical channel spacing of 600 GHz.

zoom of the WDM signal in the time domain. The five pulses presented in Fig. 3(b) are the optical pulses corresponding to each one of the five optical channels used in the WDM Ph-ADC architecture (see the signal spectrum in Fig. 3(c)). They appear separated in time due to the walk-off effect occurred along the first spool of fibre. As the WDM signal is still launched into the second spool of fibre, the impact of the walk-off on the relative delay between the optical channels is still further increased.

Fig. 4(a) depicts the time waveform corresponding to the WDM signal at the output of the second sp-ool of fibre. Fig. 4(b) shows a zoom of Fig. 4(a). Fig. 4 shows that there is a significant overlapping between the different transmitted optical pulses, i. e., the optical pulses of a given signal period that are being transmitted in one optical wavelength are overlapped (partially or totally) in time (but in the adjacent period) with the pulses carried by another wavelength. This is due to the different propagation delays of each optical channel caused by the walk-off effect along the propagation over the first and second spools of fibre. Nevertheless, as the multiplexed signals are being transmitted at different wavelengths, the optical pulses associated with each optical wavelength could still be correctly detected without additional distortion if the demultiplexing operation is performed in such a way that the crosstalk between the optical channels is avoided.

Fig. 5 shows the normalized PSD of the signals obtained at the output of the demultiplexer used in the optical receiver for the sensors corresponding to the channels transmitted at the edges and at the middle of the WDM spectrum. The PSDs of the remaining channels are not shown as they are similar to the one of Fig. 5(b). Fig. 5 shows that, even using a channel spacing of 600 GHz between the WDM channels, th-
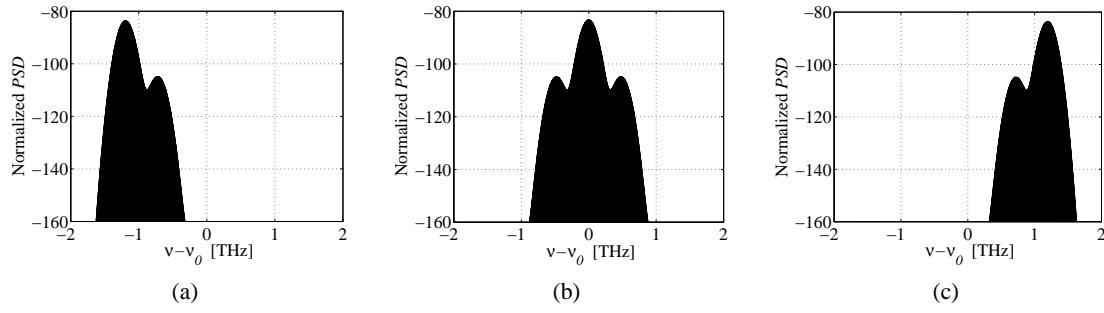
Figure 5: Normalized PSD of the demultiplexed signal at the PIN input for the sensor corresponding to the channel located at (a) one edge of the spectrum, (b) the middle of the spectrum and (c) on the other edge of the spectrum. Results obtained for an optical channel spacing of 600 GHz.
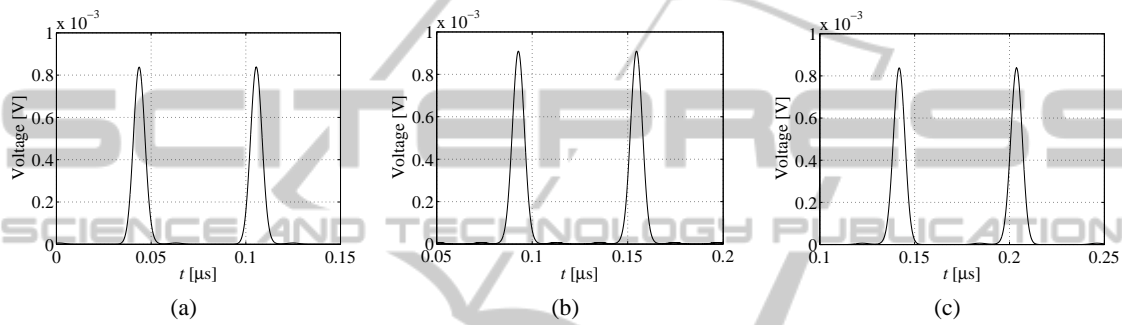

Figure 6: Zoom of the time waveforms of the signal at the PIN output for the sensor corresponding to the channel located at (a) one edge of the spectrum, (b) the middle of the spectrum and (c) on the other edge of the spectrum. Results obtained for an optical channel spacing of 600 GHz.

ere is still a small fraction of the adjacent channels in each demultiplexed signal. This crosstalk power may be of special relevance from the distortion point of view. Indeed, as the optical pulses carried by the different wavelengths may be overlapped in time due to the walk-off effect, this crosstalk power due to the adjacent channels that is not completely removed by the demultiplexing operation can lead to two different degradation effects: i) if the pulses carried by the desired wavelength and by the "crosstalk" wavelength are partially (or totally) overlapped in time, then the degradation appears as amplitude distortion and ii) if the pulses carried by the desired wavelength and by the "crosstalk" wavelength are not overlapped, then a fraction of the pulse carried by the "crosstalk" wavelength will appear in a time interval where it is not supposed to be. These conclusions have been drawn considering un-modulated optical pulses, i. e., without considering the electro-optic conversion of the radio signals captured by the sensors antennas. However, it should be stressed that the degradation effects mentioned above will lead to the same consequence when the entire WDM Ph-ADC system is working properly: the current at the output of each photo-detector provides information from the respec-

tive sensor (for instance, if the signal from sensor 1 is modulating the optical wavelength 1, the respective detected current provides information from sensor 1) and also information from the sensors that are using the adjacent wavelengths. This effect is not acceptable for adequate Ph-ADC operation as the information provided by each signal is still used by the digital signal processing algorithms and may lead to wrong (or, at least, poor) fingerprinting and localization estimates.

Fig. 6 shows a part of the time waveforms of the signals at the PIN output for the sensors corresponding to the channels located at the edges and at the middle of the spectrum (the remaining time waveforms are similar to the one of Fig. 6(b)). From the analysis of Fig. 6, it is clear that the received signal corresponding to each optical wavelength presents different peak amplitudes due to the walk-off effect, as identified above.

Fig. 7 shows results similar to the ones of Fig. 6 but considering an optical channel spacing of 400 GHz rather than 600 GHz. Fig. 7 shows that, when the channel spacing decreases, the crosstalk of the adjacent channels increases and a fraction of power appears around the desired optical pulses due
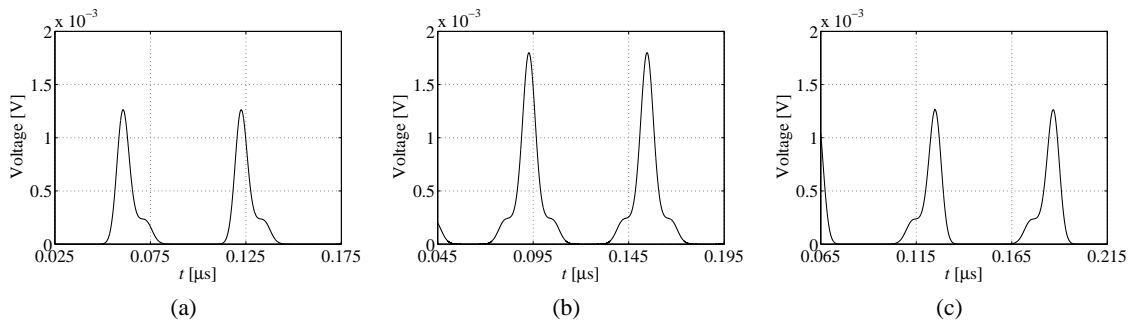
115

Figure 7: Zoom of the time waveforms of the signal at the PIN output for the sensor corresponding to the channel located at (a) one edge of the spectrum, (b) the middle of the spectrum and (c) on the other edge of the spectrum. Results obtained for an optical channel spacing of 400 GHz.
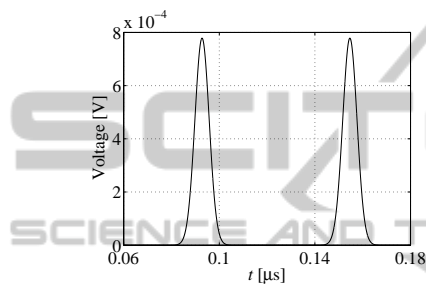

Figure 8: Zoom of the time waveform of the signal at the PIN output for the sensor corresponding to the channel located at the middle of the spectrum. Results obtained for an optical channel spacing of 800 GHz.

to the optical pulses carried by the adjacent wavelengths. Notice that, although this fraction of power only appears in one side of the pulses presented in Fig. 7(a) and 7(c), it appears in both sides of the pulses shown in Fig. 7(b) (and also in the pulses corresponding to the remaining two channels that are not presented in Fig. 7). This is because the signals depicted in Fig. 7(a) and 7(c) correspond to the channels transmitted at the edges of the WDM spectrum (suffering from the crosstalk induced by only one adjacent optical channel), while the other signals correspond to the channels transmitted at the middle of the WDM spectrum (suffering from the crosstalk induced by two adjacent optical channels). Fig. 7 shows also that the amplitude distortion effect is higher than the one observed in Fig. 6 as the crosstalk power is higher due to the tighter channel spacing used in the results of Fig. 7.

Fig. 8 depicts part of the time waveform obtained at the PIN output for the sensor corresponding to the channel located at the middle of the spectrum, considering an optical channel spacing of 800 GHz. The pulses corresponding to the remaining sensors are not shown as they are identical to the ones of Fig. 8. Fig. 8 shows that there is not any power fraction from adja-

cent optical pulses falling close to the edges of the desired pulses indicating that the crosstalk due to adjacent channels is negligible. In addition, the comparison with the pulses waveform carried by the other wavelengths showed absence of amplitude distortion as the pulses carried from the different wavelengths present similar peak amplitude levels.

Further investigation showed that the absence of signal degradation due to the walk-off effect is only reached for optical channel spacing values of the order of 800 GHz. It should be highlighted that, even with 800 GHz of channel spacing, there is time overlapping between the different pulses that comprise the WDM signal at the 2-*nd* DEMUX input. However, the impact of this effect on the different demultiplexed signals is negligible due to the absence of significant crosstalk power imposed by the adjacent optical channels. Considering this 800 GHz of channel spacing, the entire bandwidth of the multiplexed optical signal used for the WDM Ph-ADC architecture is around 5×800 GHz=4 THz and, consequently, the same bandwidth is required for the devices comprising the optical part of the WDM architecture.

4 WDM PH-ADC ARCHITECTURE OPERATION IN THE PRESENCE OF ELECTRICAL SIGNALS

In the previous section, the MUXs/DEMUXs bandwidth (400 GHz) and the optical channel spacing (800 GHz) have been chosen in order to avoid significant degradation of the optical pulses and considering that no electrical signals were modulating the optical carriers. In this section, the operation of the WDM Ph-ADC architecture considering the chosen bandwidth and channel spacing, and taking
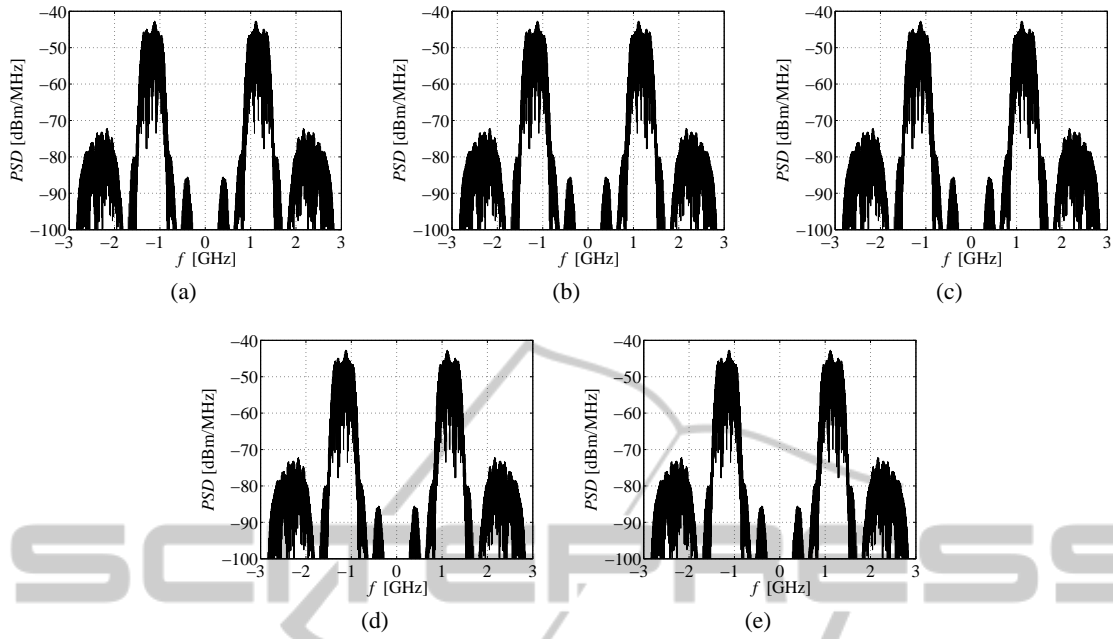
Figure 9: PSD of the time stretched received signal at the output of the BPF of each branch of the electrical receiver.
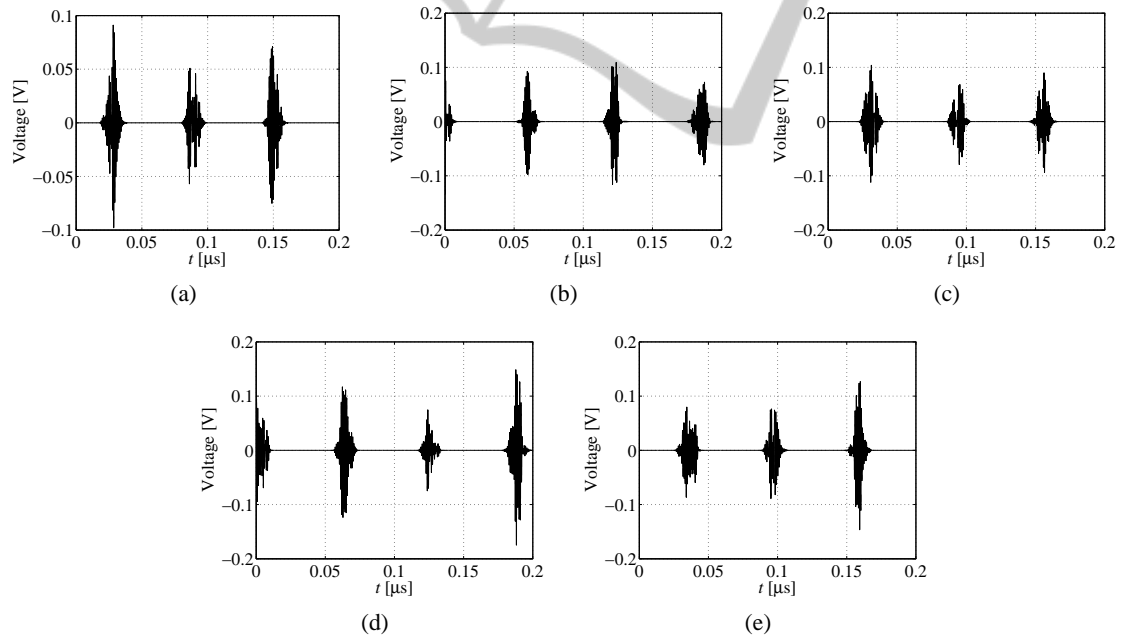

Figure 10: Time stretched received signal at the output of the BPF of each branch of the electrical receiver.

into account the signals captured by the five sensors is analyzed and discussed. The first three orthogonal frequency division multiplexing (OFDM) ultra wideband (UWB) sub-bands centred at 3.43 GHz, 3.96 GHz and 4.49 GHz are considered as the electrical signals captured by the antennas of the different sensors. The electrical mean power of the OFDM-

UWB signals at the input of the electrical sensor amplifiers is -40 dBm and an electrical amplifier gain of 40 dB is used. The gain of the optical amplifier is set 30 dB and the gain of the electrical receiver amplifiers is adjusted to 50 dB.

Fig. 9 and 10 depict the PSD and part of the time waveform of the received time stretched OFDM-

117

UWB snapshots at the output of the BPF used in each branch of the electrical receiver of the WDM Ph-ADC system. Fig. 9 and 10 confirm that time stretching of the signals at the different branches (and that have been transmitted in different optical wavelengths) of the electrical receiver is reached when the WDM architecture is employed. Notice that the OFDM-UWB radio signals centre frequency initially captured by the sensors antenna appears at the output of the WDM Ph-ADC compressed by a factor of 3.4 - the time stretching factor that is being considered. Further investigation showed that the level of the side lobes of the spectrum of the compressed signal in the WDM architecture is similar to the one obtained in the TDM architecture as it is mainly dependent only on the EOM (and the same EOM is used for both WDM and TDM approaches).

5 DISCUSSION ON THE WDM PH-ADC ARCHITECTURE PERFORMANCE

In this section, the performance comparison between the WDM and TDM Ph-ADC architectures is presented. Particularly, the signal-to-noise ratio (SNR) evaluated from the approach presented in (Alves and Cartaxo, 2011) and the degradation due to the fiber non-linearities are analyzed.

5.1 SNR

In order to compare the SNR of the WDM Ph-ADC architecture with its TDM version, let's consider that the optical peak power of each optical pulsed channel launched into the fiber in the WDM architecture is identical to the one of the TDM architecture and that the lengths of the two spools of fiber are the same in both architectures. In addition, let's consider also that the propagation in both spools of fiber can be well described as linear transmission. Within these assumptions and taking into account that the photonic structure of the WDM architecture is identical to the one of the TDM architecture, it can be concluded that, if the same electrical and optical gain levels are considered for both architectures, and that the insertion losses imposed by the MUXs/DEMUXs can be neglected, the SNR of the received signal of each branch of the WDM architecture is identical to the SNR obtained for the time stretched signal at the output of the TDM architecture. However, the insertion losses of the MUXs/DEMUXs are usually of the order of a few dB and may impose some changes on the SNR

levels obtained in the WDM architecture.

In order to assess the SNR levels obtained by both architectures, the peak SNR (Alves and Cartaxo, 2011) was evaluated for three different gain sets and considering ideal MUXs/DEMUXs (without insertion losses) and actual MUXs/DEMUXs (with insertion losses of 5 dB). The three gain sets represent situations where the total noise variance is dominantly impaired by the noise introduced by the electrical transmitter, by the optical amplifier or by the electrical receiver. In addition, the optical filter required by the TDM architecture was modeled by a Gaussian shape with a -3 dB bandwidth of 400 GHz (identical to the one of the DEMUXs/MUXs of the WDM architecture) in order to provide a fair comparison between the results. It should be stressed that, in order to have a fair comparison, also the same peak power for each optical pulsed channel launched into the fiber in the WDM architecture and in the TDM architecture has been considered. This means that the insertion losses of the AWG and of the MUX located at the input of the first spool of fiber are not relevant for the analysis.

Table 1 shows the peak SNR levels obtained for three cases: the WDM Ph-ADC considering the absence of MUXs/DEMUXs insertion losses, the WDM Ph-ADC considering MUXs/DEMUXs with insertion losses of 5 dB and the TDM Ph-ADC architecture. The results presented in Table 1 confirm that both architectures provide the same SNR performance since the system parameters are identical and MUXs/DEMUXs with negligible insertion losses are considered. However, when actual MUXs/DEMUXs are considered, the peak SNR obtained in the WDM architecture is lower than the one obtained for the TDM case. This is due to the influence of the insertion losses of the MUXs/DEMUXs on the power of the received signal and on the noise variance. In order to clarify this effect, let's analyze separately the influence of the insertion losses on each one of the three different cases of gain sets.

- **Total Noise Variance Dominantly Impaired by the Noise of the Electrical Transmitter (G_e=40 dB, G_o=30 dB, G_r=50 dB).** The total noise variance is reduced due to the insertion losses of the MUX and DEMUXs that are located at the input and at the output of the second spool of fiber, respectively. However, the signal power is further decreased by the insertion losses of the DEMUX located after the optical amplifier. Therefore, the SNR obtained for the WDM architecture is lower than for the TDM.

- **Total Noise Variance Dominantly Impaired by the Noise of the Optical Amplifier (G_e=20 dB, G_o=40 dB, G_r=50 dB).** In this case, the total noise

Table 1: Peak SNR of the TS received signal considering the WDM and TDM Ph-ADC architectures.

Peak *SNR* [dB]	G_e=40 dB G_o=30 dB G_r=50 dB	G_e=20 dB G_o=40 dB G_r=50 dB	G_e=20 dB G_o=20 dB G_r=70 dB
WDM Ph-ADC without MUXs/DEMUXs ins. losses	27	18	13
WDM Ph-ADC with MUXs/DEMUXs ins. losses	17	16	-15
TDM Ph-ADC	27	18	13

variance and the signal power are reduced by the same levels as the insertion losses of the MUX and DEMUXs of the optical link affect both in a similar way. Hence, the peak SNR obtained for the WDM architecture should be similar to the one achieved in the TDM architecture. However, as the variance due to the ASE noise contribution is reduced due to the insertion losses, the total noise variance may not be any more dominantly impaired by the noise of the optical amplifier. In this case, the peak SNR of the WDM architecture is also reduced as it will fall inside one of the two other cases.

- **Total Noise Variance Dominantly Impaired by the Noise of the Electrical Receiver (G_e=20 dB, G_o=20 dB, G_r=70 dB).** In this situation, the total noise variance is not affected by the insertion losses of the MUX and DEMUXs and thus, the SNR obtained in the WDM architecture is worse than the one achieved in the TDM as the received signal power is lower (when compared with the TDM case) due to the insertion losses.

From the study performed above it is concluded that it is not possible to obtain higher peak SNRs levels in the WDM architecture than the ones obtained for the TDM case.

5.2 Fiber Non-linearities

In order to perform a fair comparison, let's consider that the optical peak power of each optical pulsed channel of the WDM architecture is identical to the one of the optical pulsed signal used in the TDM architecture and that the pulse repetition rate of the WDM architecture is maximized (in the Ph-ADC application under analysis, it is five times higher than in the TDM case). In this situation, the total optical average power launched into the first spool of fiber is higher in the WDM architecture due to the higher pulse repetition rate. Hence, it is expected that the signals transmitted over the WDM architecture suffer from higher degradation due to the fiber non-linearities. As the channel spacing is very large

and the peak power at the optical source output can exceed 30 dBm, stimulated Raman scattering is very likely the main multi-channel non-linear impairment. The detailed quantitative assessment of the degradation induced by the fiber non-linearities of the WDM and TDM Ph-ADC architectures on the TS received signals is out of the scope of this work and will be presented elsewhere.

6 CONCLUSIONS

The performance operation of the WDM Ph-ADC architecture has been analyzed and discussed. The influence of the -3 dB MUXs/DEMUXs bandwidth and of the optical channel spacing on the WDM architecture operation has been assessed. The -3 dB bandwidth of the MUXs/DEMUXs has been chosen in order to keep the optical pulses shape at the output of those devices almost unchanged when compared with the non-filtered optical pulses. From this study, a Gaussian shape with -3 dB bandwidth of 400 GHz has been used to model the MUXs/DEMUXs. The optical channel spacing between the different optical channels has been chosen in order to have a negligible perturbation on the optical pulses due to the crosstalk induced by the optical pulses carried by the adjacent optical channels. From this study, an optical channel spacing of 800 GHz has been chosen for the WDM architecture. It has been also shown that when the proposed bandwidth and the optical channel spacing are used in the WDM architecture using five sensors, adequate time stretching of the OFDM-UWB radio signals is achieved.

In addition, it has been shown that the WDM architecture does not allow obtaining better SNR performance than the TDM architecture. It is also expected that the signals transmitted over the WDM architecture suffer from higher non-linear fiber effects than the TDM architecture.

From the study performed in this work it is concluded that if the pulse repetition rate is not of special concern for the localization and fingerprinting algo-

rithms, then the TDM architecture seems to be a better solution than the WDM counterpart.

REFERENCES

Alves, T. and Cartaxo, A. (2011). SNR approach for performance evaluation of time-stretching photonic analogue to digital converter system. *Optics Express*, 19(2):1493–1509.

Han, Y. and Jalali, B. (2003). Photonic time-stretched analogue-to-digital converter: fundamental concepts and pratical considerations. *J. Lightwave Technol*, 21(12):3085–3103.

Llorente, R., Cartaxo, A., Ugen, B., Duplicy, J., Romme, J., Puche, J., Schmertz, D., Lostanlen, Y., Banales, R., and Marti, J. (2008). Management of UWB picocell clusters: UCELLS project approach. In *Proceedings of the International Conference on Ultra-Wideband*. IEEE.

Llorente, R., Puche, M. M. J., Romme, J., and Alves, T. (2009). Sensing ultra-low-power radio signals by photonic analog-to-digital conversion. In *Proceedings of the European Conference on Optical Communications*.